Iran Polym J (2017) 26:221–228
DOI 10.1007/s13726-017-0514-4

ORIGINAL PAPER

Microstructural study of synthesized polyethylenes by homogeneous and heterogeneous nickel α-diimine catalysts

Saeid Ahmadjo[1] · Sajjad Avar[1] · Hamed Jafaraian[1] · Griselda Barrera Galland[2] · Seyed Moahammad Mahdi Mortazavi[1] · Majid Zahmaty[3]

Received: 2 October 2016 / Accepted: 6 February 2017 / Published online: 15 February 2017

Abstract In this work, ethylene polymerization was investigated by using homogeneous and heterogenouse nickel α-diimine catalysts [1,4-bis(2,6-diisopropylphenyl) acenaphthene diimine nickel(II) dibromide]. Methyl aluminoxane (MAO) and triethyl aluminum (TEA) were used as cocatalysts in homogenous and heterogeneous polymerizations, respectively. The heterogeneous catalyst showed lower activity than its homogeneous equivalent. The influence of polymerization temperature and heterogenization conditions was studied on the microstructure properties of the prepared polymers. Increasing polymerization temperature (T_P) up to 50 °C decreased the activity of both homogenous (LN) and heterogeneous (LNS) nickel α-diimine catalysts. The highest activities were 1286 and 982 kg PE (mol Ni bar h)$^{-1}$ obtained at T_P = 30 °C for LN and LNS catalysts, respectively. The polymer samples obtained by supported catalyst (LNS) showed lower unsaturation contents. Moreover, DSC analysis did not show any melting peaks for polymers obtained by LN catalyst due to their amorphous structure, which was confirmed by XRD analysis. The microstructure of the prepared polymers was completed by successive self-nucleation annealing (SSA) and was investigated by ^{13}C NMR studies. The SSA thermogram of samples made by LNS catalyst exhibited several crystal types with different lamella thicknesses. The branches in polyethylene samples produced by homogenous catalyst were higher and showed more diversity. The total methyl branch percentages for both LN and LNS catalysts were 13.1 and 3.4%, respectively.

Keywords Ethylene polymerization · Nickel α-diimine catalyst · Branching · Heterogenization · ^{13}CNMR

Introduction

Polyethylenes containing long and short branches have attracted great attention in the recent decades [1]. The existence of long branches in the polyethylene backbone improves its microstructural properties, e.g., polymer processability, toughness, impact resistance, and tensile strength [2]. Usually, Ziegler–Natta or metallocene catalysts incorporate short branches into polymers by ethylene copolymerization with α-olefin comonomers such as 1-butene, 1-hexene, and 1-octene [3, 4]. Other methods for creating branched polyethylene are based on using late-transition metal catalysts such as those reported by Svejda et al. [5], Paulovicova et al. [6], and Younkin et al. [7]. These types of catalysts have the ability to produce polymers with different microstructures in a wide range from relative linear polymers to hyper-branched or dendritic without using α-olefin co-monomers [8–10]. Special polymers can also be prepared by varying metal center and ligand type on the coordination sphere of late-transition metal catalysts [10, 11]. Late-transition metal catalysts possessing α-diimine ligands can enhance or hinder chain transfer reactions using different substitute in aryl rings. Besides, various substitutions in the *ortho*-position of the aryl ring of the catalyst may also induce the production of polyethylene with low or high degree of branching [12–14]. Heterogenization of these

✉ Seyed Moahammad Mahdi Mortazavi
m.mortazavi@ippi.ac.ir

[1] Department of Catalyst, Iran Polymer and Petrochemical Institute, P.O. Box: 14965/115, Tehran, Iran

[2] Instituto de Química, UFRGS, Av. Bento Gonçalves, 9500, Porto Alegre 91501-970, Brazil

[3] Central Laboratory, Jam Petrochemical Co., Assaluyeh, Iran

catalysts on inorganic supports, such as silica or magnesium chloride, has also been proposed to overcome some problems such as difficulty in controlling polymer morphology, relative low halftime of late-transition metal catalysts, and reactor fouling during homogenous polymerization processes [15, 16]. Several methods for immobilizing transition metal catalysts on the support have been reported in the literature including direct immobilization of catalyst on the carrier surface, grafting after support modification with MAO or alkyl aluminum compounds and finally covalent bonding of the catalyst to the support through its ligands [17]. Numerous studies have been carried out on the polymerization of the ethylene using LTM immobilized on different supports [18–20]. For instance, Chadwick et al. reported the immobilization of some of α-diimine nickel catalysts on $MgCl_2$ for ethylene polymerization [21]. In addition, the effect of $MgCl_2$ support on the morphology of the resulting polyethylene using nickel α-diimine based late transition metal catalyst was studied by Mao et al. [22]. Different immobilization methods of metallocene and late transition metal catalysts were studied in the literature [20–22]. However, there are fewer studies on polymer properties such as thermal behavior and microstructure of the obtained polymers.

In this work, we studied ethylene polymerization using both homogeneous and heterogeneous α-diimine nickel-based catalysts and the effects of heterogenization on the microstructure, and properties of the produced polyethylenes were investigated by XRD, SSA, and ^{13}C NMR techniques that have not been previously reported to this extent on this system. The novelty of this work is comprehensive microstructure study of the synthesized polyethylene samples by homogeneous and heterogeneous nickel-based (LTM) catalysts.

Experimental

Materials

Methylaluminoxane (MAO, 10 wt% solution in toluene), triethyl aluminium (TEA), and triisobutyl aluminium (TIBA) were purchased from Sigma-Aldrich (Germany). Toluene and n-heptane were provided by Bandar Imam Petrochemical Co. (BIPC, Iran). Toluene was purified by distillation over sodium wire and benzophenone, and n-heptane was dried with CaH_2 and stored over sodium wire and 4A activated molecular sieves. 2,6-Diisopropyl aniline and acenaphthenequinone were supplied by Merck (Germany). Nickel(II) dibromide salt was purchased from Sigma-Aldrich (Germany).

Catalyst and support preparation

All manipulations involving air sensitive compounds were performed under dried argon atmosphere in a glove box. LN catalyst (Scheme 1) was synthesized according to the previous report [23]. The modified support of catalyst used in this work was prepared by treating an adduct $MgCl_2{\cdot}n$EtOH (n = 3–4) (1 g) with TIBA (30 mmol) in 20 mL heptane [24]. Details of the experimental procedure for producing $MgCl_2{\cdot}n$EtOH (adduct) and modification can be found elsewhere [25, 26]. The modified support (0.1 g) was added in 5 mL toluene, to which a suitable amount of late-transition-metal catalyst (3 mmol) was added; then it was stirred for 12 h, and the precipitate was washed with toluene to give the final supported catalyst. The proposed mechanism for immobilizing of the LN catalyst over the $MgCl_2$ support is shown in Scheme 2. It is obvious that the modification of the alcoholic $MgCl_2$ by pretreatment with TIBA prepares it for the impregnation of the LN catalyst.

Polymerization

Polymerization was carried out in a 200-mL stainless steel reactor equipped with a magnetic stirrer and temperature pressure controlling systems. At first, polymerization reactor was purged with argon at 90 °C for about 2 h to ensure the absence of moisture and oxygen. Reactor was charged with 100 mL of n-heptane and purged with

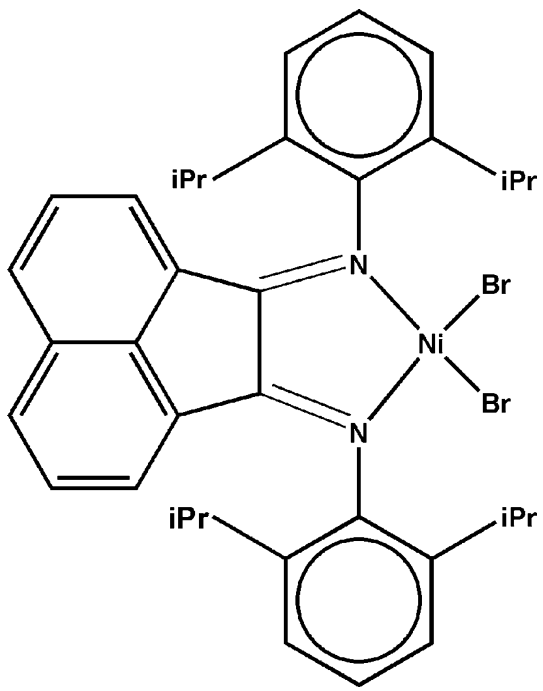

Scheme 1 Structure of Ni(II) diimine catalyst

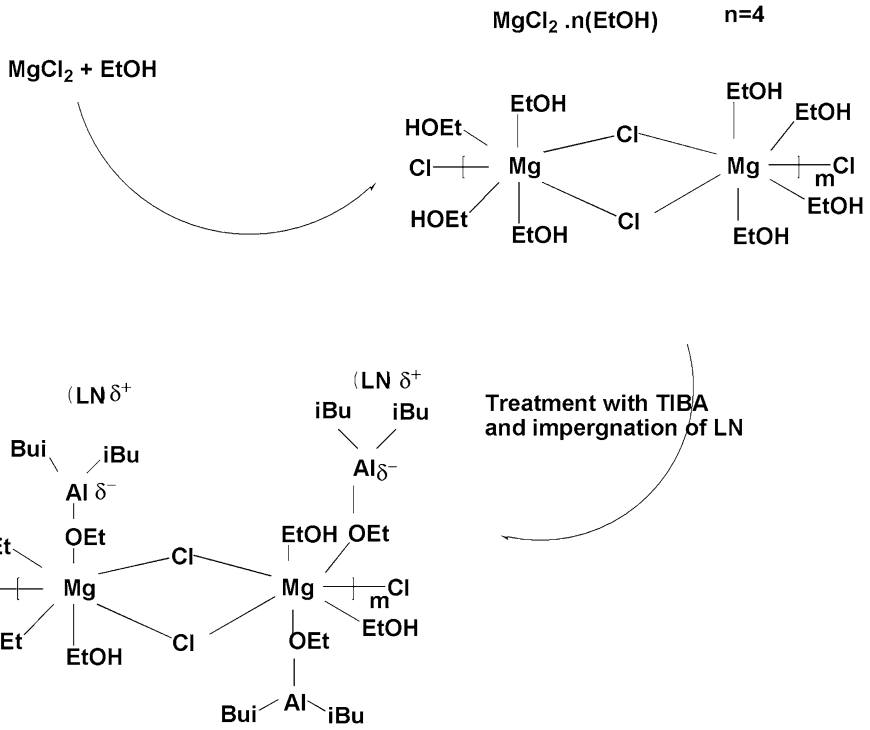

Scheme 2 Proposed mechanism for immobilizing of LN catalyst over $MgCl_2$ support, (iBu: isobutyl)

ethylene and temperature was adjusted to the polymerization temperature, subsequently. Methyl aluminoxane (MAO) in the homogeneous and triethyl aluminium (TEA) in the heterogeneous polymerizations were used and then the catalysts were added to the polymerization reactor. Polymerization was started by setting the ethylene pressure in reactor. After 30 min, polymerization was stopped and ethylene was discharged from the reactor. The obtained polymers were washed with acidified methanol and dried under vacuum oven.

Characterization

The viscosity average molecular weights (M_v) of polymers were determined in decahydronaphthalene at constant temperature 135 ± 0.1 °C using Ubbelohde viscometer and Mark–Houwink–Sakurada equation [27]. Fourier transform infrared spectroscopy (FTIR) experiments were carried out with a FTIR Bruker-IFS 48 (Germany) spectrophotometer. Vibrational bands of polymer structures in the range of 4000–500 cm^{-1} were analyzed. For calculating unsaturation percentage for polyethylene samples, the peak area corresponding to vinyl group absorptions in the 910–908 and 2019 cm^{-1} regions were measured and the percentage of vinyl end groups calculated using the obtained Eq. (1) from the calibration curve [28]:

$$C = C\ (\%) = (2.751 \times [A_{908}/A_{2019}] - 0.111) \times 100. \quad (1)$$

Differential scanning calorimetry (DSC) curves of the polymers were obtained by applying Mettler-Toledo (823e, Switzerland) instrument. Samples were heated from room temperature to 150 °C at the rate of 10 °C min^{-1} under nitrogen gas flow. Then, the system was kept for 10 min at the same temperature, followed by cooling to 25 °C by the rate 10 °C min^{-1}. Finally, samples were heated from 25 to 150 °C with the same heating rate, and the final DSC curves were collected at the last heating cycle. Lamella thickness and heterogeneity index were calculated with successive self-nucleation and annealing (SSA) as described in previous work [29]. X-ray powder diffraction (XRD) was used to observe crystal content of the polyethylene samples using a Siemens D5000 X-Ray (Germany) diffractometer. Branching contents of the polymers were measured using a Varian Inova 300 (USA) NMR spectrometer, operating at 75 MHz. Samples were dissolved in the *ortho*-dichlorobenzene and deuterated benzene (20% v/v) and ^{13}C NMR spectra were collected at 120 °C and consequently the branching data were calculated according to previous reports [30, 31].

Results and discussion

Catalyst activity

Results of homogeneous (LN) and heterogeneous (LNS) late-transition metal catalyst activities at different

Table 1 Ethylene polymerization using LN and LNS catalysts

Catalyst code	T_P (°C)	Activity (kg PE (mol M bar h)$^{-1}$)	M_v (kg mol^{-1})	Unsaturation (%)[c]	T_m (°C)	X_C^d (%)
LN[a]	30	1286	511	–	–[e]	–
LN	50	966	365	4.7	–	–
LN	70	583	317	–	–	–
LNS[b]	30	982	1687	–	120	21
LNS	50	650	828	4.4	103	19
LNS	70	325	359	–	122	14

Polymerization conditions: ethylene pressure: 4 bar, catalyst concentration [M] = 3 μmol (LN), [M] = 2.16 μmol (LNS) determined by ICP, polymerization time: 30 min, heptane: 100 mL

[a] MAO: 4 mmol

[b] TEA: 4 mmol

[c] Determined by FTIR

[d] Measured by DSC, Crystallinity based on $\Delta H_m = 293$ J g^{-1} for a 100% crystalline PE

[e] The polymers were totally amorphous

polymerization temperatures are shown in Table 1. The results showed that by increasing T_P, the catalyst activity decreased probably due to phenomena such as possible changes in the structure of catalyst or the lower solubility of the monomer in the polymerization medium at higher T_P [9, 32]. However, Xu et al. [22] and Schilling et al. [33] reported some heterogeneous LTM catalysts that exhibited higher polymerization activities than the corresponding homogeneous LTM catalysts. In contrast, Jiang et al. [17] reported drop in the activity of supported LTM catalyst by increasing the polymerization temperature. Therefore, prediction of the polymerization activities in heterogeneous catalysts is difficult due to the complexity of their structures or properties of the supports that were used.

The highest activity 1286 kg PE (mol Ni bar h)$^{-1}$ was obtained at $T_P = 30$ °C in the homogeneous system. Comparing with the LN catalyst, the LNS showed lower activity at the same polymerization condition. This effect might be probably due to deactivation of some active sites during the grafting reaction or even due to the steric effect of the support itself that plays the role of a huge ligand [15, 22]. The highest activity for LNS catalyst was observed at $T_P = 30$ °C, similar to LN catalyst (Table 1).

The results of Table 1 showed that M_v of the resultant polymers obtained by LN and LNS catalysts decreased with increasing polymerization temperature under the same polymerization condition. This effect can be due to the enhancement of chain transfer rates or to the increase in termination over propagation reactions at the higher temperature, making it more difficult to produce polymers with high molecular weights [16]. Moreover, supported catalyst led to higher M_v in comparison to LN catalyst probably due to lower β-hydride elimination reactions (Table 1) [34, 35]. Ma et al. synthesized silica-supported iron (LTM) catalyst for ethylene polymerization: this catalyst produced polymers with higher molecular weights and melting temperatures compared to unsupported catalyst [19]. In general, the probability of occurring β-hydride elimination reactions in late transition metal catalysts is high. This type of termination reaction produces polymers with an unsaturated terminal chain (vinyl or vinylidene terminal groups), while chain transfer to aluminum gives completely saturated polymer chains. Vinyl terminated chains were capable of re-insertion into the main chain to form long branches that is characters of polymers obtained by LTM catalyst [35]. According to Table 1, at $T_P = 30$ °C the unsaturation percentage in polymer chains using LNS catalyst decreased from 4.7 to 4.4 compared with LN catalyst. This behavior can be attributed to lower β-hydride elimination reactions upon heterogenization as confirmed by M_v results [15, 17]. Kaminsky et al. [36] reported unsaturation percentage between 6.8 and 17% for polymers obtained by bridged metallocene catalysts.

Thermal properties of polymers

The effect of polymerization temperature on thermal properties of the polymers obtained with LNS catalyst was investigated by DSC analysis. As shown in Fig. 1, at $T_P = 30$ °C a sharp melting peak at 120 °C was obtained which was evolved into two broad peaks at 117 °C and 103 °C for $T_P = 50$ °C. The broadening of the peak at this polymerization temperature may be probably due to higher branching associated with the enhancement of the chain walking or could be attributed to more irregularity of the chain structure that possessed different branch densities in the prepared polyethylene. Moreover, at $T_P = 70$ °C only a melting peak at 122 °C and the drop in activity can be seen (Table 1). Higher melting points are attributed to the chains with fewer number of branches [15, 37]. Alobaidi et al. also reported that increasing polymerization temperature led to a decrease in the polymers melting temperature obtained by

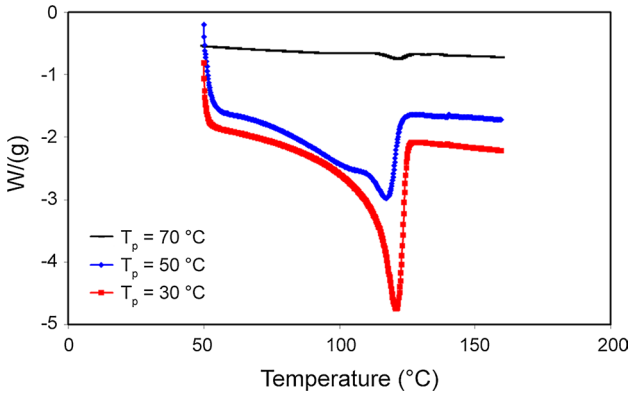

Fig. 1 DSC thermograms for produced PE samples using LNS catalyst

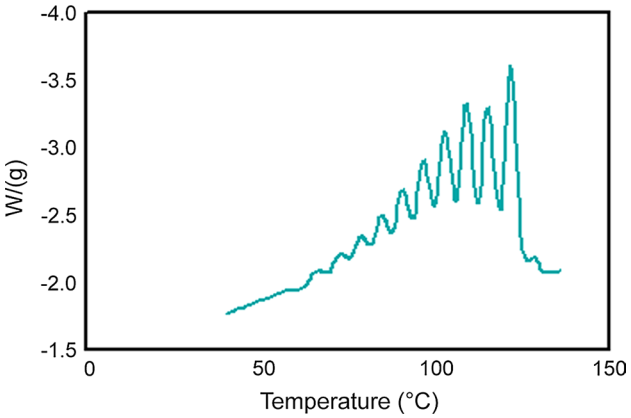

Fig. 2 SSA thermograms for produced PE sample using LNS catalyst at $T_P = 50$ °C

homogenous LTM catalyst; this trend showed a reduction in the short chain branch contents [15].

The polymer obtained with LN catalyst was amorphous and did not show any melting peak, which can be attributed to the production of the highly branched polyethylene [38]. This observation confirmed that catalyst heterogenization decreased chain walking to a great extent [20, 21, 37]. The crystallinity contents of the polymers made by LNS catalyst decreased as polymerization temperature increased. In other words, the extent of branching increased with polymerization temperature (Table 1; Fig. 2). Jiang et al. [17] produced branched polyethylene by α-diimine catalyst covalently supported on SiO_2 and $MgCl_2$ at higher polymerization temperature. In contrast, Choi et al. [39] synthesised a clay (MMT)-supported (LTM) catalyst that produced polyethylene with high melting temperature due to reduction in the chain walking reaction. Therefore, different steric effects are available in the supported catalysts, resulting in either improvement or reduction of chain walking reaction which leads to formation of more amorphous or more crystalline polyethylene, respectively [37, 39].

Successive self-nucleation annealing (SSA) analysis is a rapid and practical approach for assessing chain heterogeneity in polyolefins. The synthesized polymers using LNS catalyst showed several peaks (Fig. 2), which suggest the existence of polyethylene with various crystal sizes and lamella thicknesses. The multiplicity of the endotherm peak is related to different lamellar thicknesses of the obtained polyethylene, which may be due to different branch contents [40]. It is also observed that the lamella thickness distribution specified by DSCI criteria (Table 2) approaches one, which is similar to the behavior of metallocene catalyzed PE [40, 41]. No peak was observed for homogeneous sample obtained by LN catalyst. This clearly showed the catalyst forms highly branched and, therefore, amorphous polymer. The lamellar thicknesses and heterogeneity index values are shown in Table 2. The melting temperature is related to the branch content and increasing the branch content decreases lamellar thickness of the crystal structure and thus lowers melting temperature [15, 37].

Crystallinity of polymers

X-ray diffraction analysis (XRD) of the polymers obtained by LN and LNS catalysts at polymerization temperature of 50 °C is depicted in Fig. 3. As seen in this figure, XRD pattern of the obtained PE using LNS catalytic system shows two diffraction peaks corresponding to (110) and (200); sharp peaks are due to scattering from crystalline regions. On the other hand, the polymer obtained by LN catalyst presents only a broad peak that corresponds to the scattering from non-crystalline structures. Ray et al. used clay as a support for Fe-based diimine catalysts; the produced polyethylene exhibited crystalline region in the

Table 2 Lamella thicknesses and heterogeneity index value of the obtained PE using LNS catalyst at $T_P = 50$ °C

Peak no.	L_c (nm)	T_m (°C)	DSCI[a]
1	2.6	67	0.57
2	2.82	73	0.61
3	3.08	79	0.64
4	3.38	85	0.69
5	3.76	91	0.74
6	4.23	97	0.79
7	4.84	103	0.86
8	5.64	109	0.91
9	6.77	115	0.90
10	8.83	122	1.00

[a] DSCI (heterogeneity index) can be obtained from any peak height toward tallest peak height

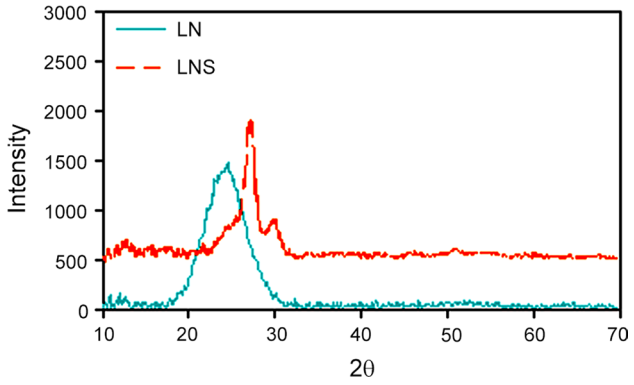

Fig. 3 XRD patterns of produced PE samples using LN and LNS catalysts at $T_P = 50$ °C

XRD pattern [42]. The obtained results showed that LNS catalyst produces higher crystalline polymers than LN catalyst; accordingly LNS catalyst produces polymers with lower branching content due to lower chain walking reaction. While, the LN catalyst prevents effective crystallization of polyethylene due to excessive branching [43, 44].

Branching contents determined by ^{13}C NMR

The correlation of molecular structure and physical properties has to be taken into account for providing a correct analysis of branching in polyethylene. ^{13}C NMR is undoubtedly the best technique to investigate the microstructure of these materials, and it has been extensively used to characterize branching in polymers. In the present research, the amount and type of branches in the obtained polymers were analyzed by means of ^{13}C NMR spectroscopy (Table 3). Calculations and measurements based on peak integration were done according to the method proposed by Galland et al. [30, 31].

As can be seen in Fig. 4, the signals of the methyl branches and the methine carbon were observed near 20 and 33 ppm, respectively. The paired 1,4 methyl branches and 1,5 and 1,6 methyl branches were identified by the presence of the resonance peaks at 34.7, 24.6, and 27.8 ppm, respectively [2, 30, 31]. The long-chain branch (N_L) was observed by the presence of peaks at 32.16 and 29.59 ppm, for polymer obtained with LN catalyst (sample A). The results in Table 3 show that the polymer obtained by LN catalyst includes mainly methyl and long branches. Alobaidi et al. [15] showed that the typical homogeneous α-diimine catalysts produced polyethylene with the higher methyl branches compared to long branches. Jiang et al. [17] also used heterogeneous LTM catalyst for synthesis of the branched polyethylene, however, a linear semi-crystalline polyethylene was obtained at 0 °C, and the ^{13}C NMR spectrum of the obtained polymer showed just the signal for methyl branches. By increasing the polymerization temperature, methyl branch decreased but longer branch and degree of branching increased. The total amount of methyl branches for polymers obtained by LN and LNS catalysts were 13.2 and 3.4%, respectively. Polymer obtained by LNS catalyst showed lower amount of branches than the one obtained by LN catalyst, which mainly was constituted by methyl branches. Ye et al. [37] reported that MCM supported LTM catalyst produced branched polyethylene, although its short chain branches were less than those produced by the

Table 3 Short and long chain branching distribution of PE made with LN and LNS catalysts at $T_P = 50$ °C

Branch type	Sample			
	LN		LNS	
	Percentage over total branching (%)	Percentage over main chain (%)	Percentage over total branching (%)	Percentage over main chain (%)
N_M (isolated)	4.4	25.9	1.8	54.9
$N_{M(1,4)}$	1.0	6.2	0.5	16.1
$N_{M(1,5)}$	2.3	13.4	0.0	0.0
$N_{M(1,6)}$	5.4	31.6	1.0	29.0
Total N_M	13.1	77.0	3.4	100.0
N_E	0.6	3.7	0.0	0.0
N_P	0.9	5.3	0.0	0.0
N_B	1.2	7.2	0.0	0.0
N_a	0.0	0.0	0.0	0.0
N_L (isolated)	1.1	6.7	0.0	0.0
$N_{L(1,4)}$	0.0	0.00	0.0	0.0
Total N_L	1.1	6.2	0.0	0.0
Total branches	18.0	100.0	3.4	100.0

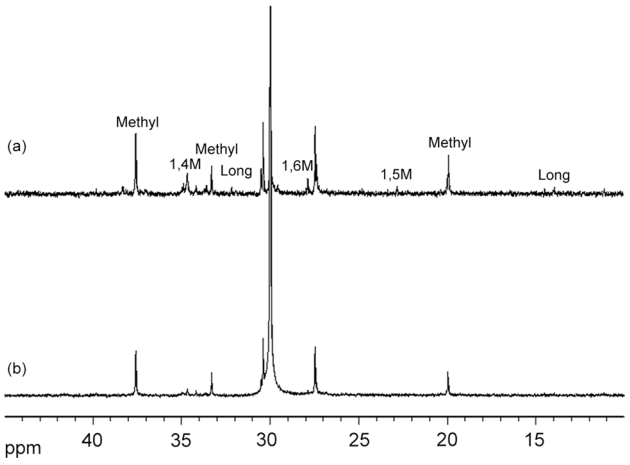

Fig. 4 ^{13}C NMR spectra of synthesized polyethylenes using LN (**a**) and LNS (**b**) catalysts

homogeneous LTM catalyst. These results are in accordance with the SSA results that the heterogenization of LTM catalysts leads to lower chain walking and β-hydride elimination due to steric hindrance of the support structure [45, 46].

Conclusion

Ethylene polymerization was carried out using homogeneous and heterogeneous nickel α-diimine catalysts. The heterogeneous catalyst showed lower activity than homogeneous catalyst. Viscometer measurements and FTIR results demonstrated that heterogeneous catalyst (LNS) produced higher M_v and lower unsaturation content than homogeneous catalyst (LN). The study of thermal properties of the prepared polymers using DSC analysis revealed that supported catalyst (LNS) enhanced crystallinity but for (LN) catalyst no melting peak was observed which was confirmed by XRD results. Furthermore, SSA thermogram of samples made by LNS catalyst exhibited several crystal types with different lamellar thicknesses. ^{13}C NMR analysis showed that LNS catalyst could produce polyethylene containing relatively low branches compared with LN catalyst. For both catalysts, methyl branches were dominant.

References

1. Hoff R, Mathers RT (eds) (2010) Handbook of transition metal polymerization catalysts. John Wiley, Hoboken
2. Hustad PD, Kuhlman RL, Shan CLP (2012) Chain shuttling catalysis and olefin block copolymers. In: Matyjaszewski K, Möller M, Elsevier BV (eds) Polymer science: a comprehensive reference, vol. 3. Elsevier, Amsterdam, pp 699–737
3. Wannaborworn M, Praserthdam P, Jongsomjit B (2011) Observation of different catalytic activity of various 1-olefins during ethylene/1-olefin copolymerization with homogeneous metallocene catalysts. Molecules 16:373–383
4. Yang H, Zhang L, Fu Z, Fan Z (2015) Comonomer effects in copolymerization of ethylene and 1-hexene with $MgCl_2$-supported Ziegler–Natta catalysts: new evidences from active center concentration and molecular weight distribution. J Appl Polym Sci 132:41264–41268
5. Svejda SA, Johnson LK, Brookhart M (1999) Low-temperature spectroscopic observation of chain growth and migratory insertion barriers in (α-diimine) Ni(II) olefin polymerization catalysts. J Am Chem Soc 121:10634–10635
6. Paulovicova A, El-Ayaan U, Shibayama K, Morita T, Fukuda Y (2001) Mixed-ligand copper(II) complexes with the rigid bidentate Bis(*N*-arylimino) acenaphthene ligand: synthesis, spectroscopic and X-ray structural characterization. Eur J Inorg Chem 10:2641–2646
7. Younkin TR, Connor EF, Henderson JI, Friedrich SK, Grubbs RH, Bansleben DA (2000) Neutral, single-component nickel (II) polyolefin catalysts that tolerate heteroatoms. Science 287:460–462
8. Johnson LK, Killian CM, Brookhart M (1995) New Pd(II)- and Ni(II)-based catalysts for polymerization of ethylene and α-olefins. J Am Chem Soc 117:6414–6415
9. Gates DP, Svejda SA, Oñate E, Killian CM, Johnson LK, White PS, Brookhart M (2000) Synthesis of branched polyethylene using (α-diimine) nickel(II) catalysts: influence of temperature, ethylene pressure, and ligand structure on polymer properties. Macromolecules 33:2320–2334
10. Khoshsefat M, Ahmadjo S, Mortazavi SMM (2016) Reinforcement effects of nanocarbons on catalyst behaviour and polyethylene properties through in situ polymerization. RSC Adv 6:88625–88631
11. McCord EF, McLain SJ, Nelson LTJ, Arthur SD, Coughlin EB, Ittel SD (2001) ^{13}C and 2D NMR analysis of propylene polymers made with α-diimine late metal catalysts. Macromolecules 34:362–371
12. Khoshsefat M, Zohuri GH, Ramezanian N, Ahmadjo S, Haghpanah M (2016) Polymerization of ethylene using a series of binuclear and a mononuclear Ni(II)-based catalysts. J Polym Sci Polym Chem 54:3000–3011
13. Camacho DH, Salo EV, Ziller JW, Guan Z (2004) Cyclophane-based highly active late-transition-metal catalysts for ethylene polymerization. Angew Chem Int Ed 43:1821–1825
14. Camacho DH, Guan Z (2010) Designing late-transition metal catalysts for olefin insertion polymerization and copolymerization. Chem Commun 46:7879–7893
15. Alobaidi F, Ye Z, Zhu S (2004) Ethylene polymerization with homogeneous nickel–diimine catalysts: effects of catalyst structure and polymerization conditions on catalyst activity and polymer properties. Polymer 45:6823–6829
16. Choi Y, Soares JBP (2012) Supported single-site catalysts for slurry and gas-phase olefin polymerisation. Can J Chem Eng 90:646–671
17. Jiang H, Lu J, Wang F (2010) Polymerization of ethylene using a nickel α-diimine complex covalently supported on SiO_2–$MgCl_2$ bisupport. Polym Bull 65:767–777
18. Schrekker HS, Kotov V, Preishuber-Pflugl P, White P, Brookhart M (2006) Efficient slurry-phase homopolymerization of ethylene to branched polyethylenes using α-diimine nickel(II) catalysts covalently linked to silica supports. Macromolecules 39:6341–6354
19. Ma Z, Sun W-H, Zhu N, Li Z, Shao C, Hu Y (2002) Preparation of silica-supported late transition metal catalyst and ethylene polymerization. Polym Int 51:349–352

20. Huang R, Liu D, Wang S, Mao B (2005) Preparation of spherical $MgCl_2$ supported bis(imino)pyridyl iron(II) precatalyst for ethylene polymerization. J Mol Catal A Chem 223:91–97
21. Severn JR, Chadwick JC, Casteli VVA (2004) $MgCl_2$-based supports for the immobilization and activation of nickel diimine catalysts for polymerization of ethylene. Macromolecules 37:6258–6259
22. Xu R, Liu D, Wang S, Mao B (2006) Preparation of spherical $MgCl_2$-supported late-transition metal catalysts for ethylene polymerization. Macromol Chem Phys 207:779–786
23. Arabi H, Ghafari M, Zohuri GH, Damavandi S (2013) Polymerization of ethylene using α-diimine nickel catalyst. Iran J polym Sci Tech 26:327–335 **(in Persian)**
24. Ahmadi M, Jamjah R, Nekoomanesh M, Zohuri GH, Arabi H (2007) Ziegler–Natta/metallocene hybrid catalyst for ethylene polymerization. Macromol React Eng 1:604–610
25. Jamjah R, Zohuri GH, Vaezi J, Ahmadjo S, Nekomanesh M, Pouryari M (2006) Morphological study of spherical $MgCl_2{\cdot}n$EtOH supported $TiCl_4$ Ziegler–Natta catalyst for polymerization of ethylene. J Appl Polym Sci 101:3829–3834
26. Ahmadjo S, Dehghani S, Zohuri GH, Nejabat GR, Jafarian H, Ahmadi M, Mortazavi SMM (2015) Thermal behavior of polyethylene reactor alloys polymerized by Ziegler–Natta/late transition metal hybrid catalyst. Macromol React Eng 9:8–18
27. Ahmadjo S, Arabi H, Zohuri G, Nekoomanesh M, Nejabat G, Mortazavi SMM (2014) Preparation of ethylene/α-olefins copolymers using (2-RInd)2ZrCl2/MCM-41 R:Ph, H) catalyst, microstructural study. J Therm Anal Calorim 116:417–426
28. Britovsek GJP, Bruce M, Gibson VC, Kimberley BS, Maddox PJ, Mastroianni S, McTavish SJ, Redshaw C, Solan GA, Strömberg S, White AJP, Williams DJ (1999) Iron and cobalt ethylene polymerization catalysts bearing 2,6-bis(imino)pyridyl ligands: synthesis, structures, and polymerization studies. J Am Chem Soc 121:8728–8740
29. Mortazavi SMM, Arabi H, Zohuri GH, Ahmadjo S, Nekoomanesh M, Ahmadi M (2009) Ethylene homo- and copolymerization using a bis-Ind$ZrCl_2$ metallocene catalyst: structural composition distribution of the copolymer. Macromol React Eng 3:263–270
30. Galland GB, Desouza RF, Mauler RS, Nunes FF (1999) ^{13}C NMR Determination of the composition of linear low-density polyethylene obtained with [η3-methallyl-nickel-diimine]PF_6 complex. Macromolecules 32:1620–1625
31. Galland GB, Quijada R, Rojas R, Bazan G, Komon ZJA (2002) NMR study of branched polyethylenes obtained with combined Fe and Zr catalysts. Macromolecules 35:339–345
32. Pourtaghi-Zahed H, Zohuri GH (2013) Polymerization of propylene catalyzed by α-diimine nickel complexes/methylaluminoxane: catalytic behavior and polymer properties. Polym Bull 70:1769–1780
33. Schilling M, Bal R, Görl C, Alt HG (2007) Heterogeneous catalyst mixtures for the polymerization of ethylene. Polymer 48:7461–7475
34. Köppl A, Alt HG (2000) Substituted 1-(2-pyridyl)-2-azaethene-(*N*,*N*)-nickel dibromide complexes as catalyst precursors for homogeneous and heterogeneous ethylene polymerization. J Mol Catal A Chem 154:45–53
35. O'Reilly ME, Dutta S, Veige AS (2016) β-Alkyl elimination: fundamental principles and some applications. Chem Rev 116:8105–8145
36. Arikan B, Kaminsky W (2005) Synthesis of long-chain branched polyethylene with ethylene/propylene co-monomer side chains. Design Monomer Polym 8:539–600
37. Ye Z, Alsyouri H, Zhu S, Lin YS (2003) Catalyst impregnation and ethylene polymerization with mesoporous particle supported nickel–diimine catalyst. Polymer 44:969–980
38. Simon LC, DeSouza RF, Soares JBP, Mauler RS (2001) Effect of molecular structure on dynamic mechanical properties of polyethylene obtained with nickel–diimine catalysts. Polymer 42:4885–4892
39. Choi YS, Shin SYA, Soares JBP (2010) Preparation of polyethylene/montmorillonite nanocomposites through in situ polymerization using a montmorillonite-supported nickel diimine catalyst. Macromol Chem Phys 211:1026–1034
40. Mortazavi SMM, Arabi H, Zohuri GH, Ahmadjo S, Nekoomanesh M, Ahmadi M (2010) Copolymerization of ethylene/α-olefins using bis(2-phenylindenyl)zirconium dichloride metallocene catalyst: structural study of comonomer distribution. Polym Int 59:1258–1265
41. Zhang M, Wanke SE (2003) Quantitative determination of short-chain branching content and distribution in commercial polyethylenes by thermally fractionated differential scanning calorimetry. Polym Eng Sci 43:1878–1888
42. Ray S, Galgali G, Lele A, Sivaram S (2005) In situ polymerization of ethylene with bis(imino)pyridine iron(II) catalysts supported on clay: the synthesis and characterization of polyethylene–clay nanocomposites. J Polym Sci Polym Chem 43:304–318
43. Li W, Wang J, Jiang B, Yang Y, Jie Z (2010) Ethylene polymerization with hybrid nickel diimine/Cp_2TiCl_2 catalyst: a new method to prepare blends of linear and branched polyethylene. Polym Int 59:617–623
44. Li K-T, Dai C-L, Kuo C-W (2007) Ethylene polymerization over a nano-sized silica supported Cp_2 $ZrCl_2$/MAO catalyst. Catal Commun 8:1209–1213
45. Jiang H, He F, Wang H (2009) A new strategy to prepare branching polyethylene by using an α-diimine nickel(II) complex covalently supported on $MgCl_2$/AlRn$(OEt)_{3-n}$. J Polym Res 16:183–189
46. Zou H, Zhu FM, Wu Q, Ai JY, Lin SA (2005) Synthesis of long-chain-branched polyethylene by ethylene homopolymerization with a novel nickel(II) α-diimine catalyst. J Polym Sci Polym Chem 43:1325–1330